

Flow rate effect on droplet control in a co-flowing microfluidic device

Yiping Hong · Fujun Wang

Received: 21 September 2006 / Accepted: 31 October 2006 / Published online: 30 November 2006
© Springer-Verlag 2006

Abstract Flow rate effect on droplet formation in a co-flowing microfluidic device is investigated numerically. Transition conditions are discovered that the droplet size is either approximately independent of or strongly dependent on the flow rate ratio. This phenomenon is explained by the relation between strain rate and droplet diameter. Regions of four drop patterns are demarcated and conditions that give polydisperse drops are described, which is helpful to assure the accuracy and efficiency in droplet production.

Keywords Microdroplet · Monodisperse · Flow rate effect · Droplet patterns · Co-flowing system

1 Introduction

Droplet formation in immiscible fluids has applications in many fields including pharmaceuticals, biology, foods and cosmetics. Microdroplets can be generated in microfluidic devices. Emulsions were formed by colliding streams of immiscible fluids at a T-shaped junction (Thorsen et al. 2001). Alternatively, when a small orifice was placed at a certain distance downstream of coaxial inlet streams, dispersions were formed using this focusing geometry (Garstecki et al. 2005). Other flow-focusing techniques that produced monodisperse droplets exist (Ganan-Calvo et al. 2001). Drops were formed when the disperse phase was injected via a needle or tube into another co-flowing

immiscible fluid (Cramer et al. 2004). Each of the above techniques has its own advantage and drop formation mechanism. The initial study on this topic has been mainly experimental. While drop formation is also an interesting topic in numerical study. The volume of fluid/continuous surface force method was used to investigate the jet dynamics with the Reynolds number exceeding 400 (Richards et al. 1995). Evolution of drop profiles and formation of satellite drops from a tube of radius = 0.16 cm were shown with the finite difference algorithm (Zhang 1999). Bubble and droplet formation in microfluidic devices have been recently reported using the finite element method (Jensen et al. 2006; Suryo et al. 2006). To aid design of microfluid devices, flow rate effect on droplet control needs to be studied in detail.

Microfluidic devices can produce monodisperse droplets with a low coefficient of variation ($CV < 5\%$) of the diameter (Nisisako et al. 2003). Droplet sizes can be tuned by adjusting the input flow rates. Unfortunately, this affects simultaneously the frequency, size, composition, speed of the droplets (Joanicot et al. 2005), as well as the complex patterns. These patterns range from periodic monodisperse droplets to polydisperse “ribbons” (Thorsen et al. 2001) and “pearl necklace” (Dreyfus et al. 2003), etc., which bring difficulty to the control process. In order to improve and optimize the design, regions for different drop patterns need to be demarcated, which is investigated in this study.

Experimental study on ordered and disordered patterns in “planar” microfluidic systems was presented by Dreyfus et al. (2003), in which microchannels were fabricated on a planar substrate. Their system formed a crosslike (T type) injection configuration. While we now report the numerical study on the

Y. Hong (✉) · F. Wang
Department of Fluid Machinery and Fluid Engineering,
China Agricultural University, Beijing 100083, China
e-mail: yphong@cau.edu.cn

droplet breakup in a coaxial microcapillary device with the co-flowing system. Patterns of drops, pears and pearl necklaces were presented in Dreyfus's study, these patterns were demarcated mainly by different shapes. We now use the coefficient of variation to describe the patterns in our study. Two major new findings in our present work will be given in [Results and discussion](#) below. As the presentation of the result in dimensional form limits its validity and application, the different flow regimes in our study are given in a dimensionless framework.

This paper presents a numerical study on the flow rate effects on droplet formation. In part two, the numerical model is described. In part three, numerical results and discussion are presented. General flow rate effects are given in Fig. 1. Flow rate effects in the regime of $Q_d/Q_c \geq 0.1$ are given in Fig. 2. Flow rate effects in the regime of $Q_d/Q_c < 0.1$ are given in Fig. 3.

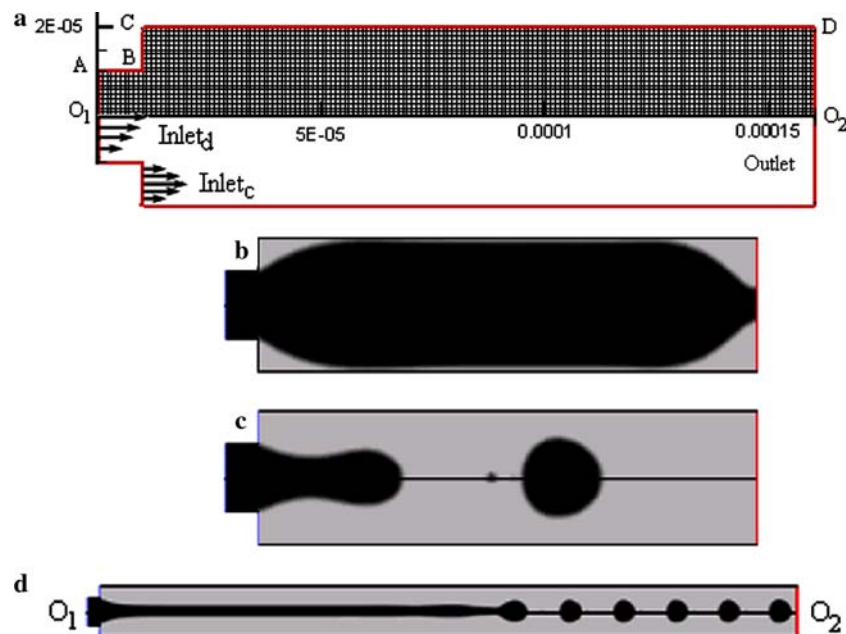
2 Numerical model

A disperse phase (viscosity $\mu_d = 1.0$ mPa s, density $\rho_d = 1,000$ kg/m³) flows from an inner tube into a larger pipe, which is filled with the continuous phase (viscosity $\mu_c = 3.32$ mPa s, density $\rho_c = 830$ kg/m³). Their interfacial tension is $\sigma = 15$ mN/m. Gravity is directed toward the flowing direction. The tube diameter (d_t) and the pipe diameter (d_p) are 20 and 40 μm , respectively. Microfluidic devices with diameters of 8–20 μm in smooth walled cylindrical channels can be fabricated using the laser method (Day et al. 2005). The geometry and grids for this axisymmetric flow are shown in

Fig. 1a. O_1O_2 is the axis (160 μm). AB and CD are, respectively, boundaries of the coaxial tube and pipe. The contact angle is 180° , complex effects of surface roughness on droplet size (Li 1996) are not considered in this study. The no-slip boundary condition is used, as it remains an excellent approximation for flows at scales above micrometers (Stone et al. 2004; Gadelhak 2000). O_1A and BC are set as velocity inlets of the disperse phase and the continuous phase, respectively. O_2D is set as a pressure outlet of the mixture. Volume of fluid method is used for tracking the interface of two immiscible fluids, using a multiphase model in the commercial software FLUENT. The iteration time step size is 10^{-7} second and the convergence criterion is 10^{-6} for each variable. Grids with the interval size of (1 μm) are used in numerical simulations. Finer grids with the interval size of (0.5 μm) have been tested and the difference between these two predicted droplet diameters is less than 1% after convergence.

Droplet generation is achieved by high shear forces generated at the leading edge of the disperse phase. Competition between surface tension and shear forces results in droplet formation, while many important variables can affect droplet size and each can be used for droplet optimization. These variables are summarized as channel structure (such as type and dimension), fluid properties (such as density, viscosity, surface tension and wall contact angle), and operating parameters (such as pressure, flow rate ratio and average velocity). Only operating parameters are discussed in this paper. Fluid properties have been described above and the channel structure is shown in Fig. 1a.

Fig. 1 Flow channel and drop formation. **a** Grids and boundary of the geometry, **b** laminar flow with $Ca = 0$ and $Re = 4$. **c** Discrete droplets with $Ca = 0.111$ and $Re = 4$. **d** Droplets formation with $Ca = 0.221$ and $Re = 6$. The suspended column of the disperse fluid at the tube is about $8d_p$. The structure length (O_1O_2) is $14d_p$



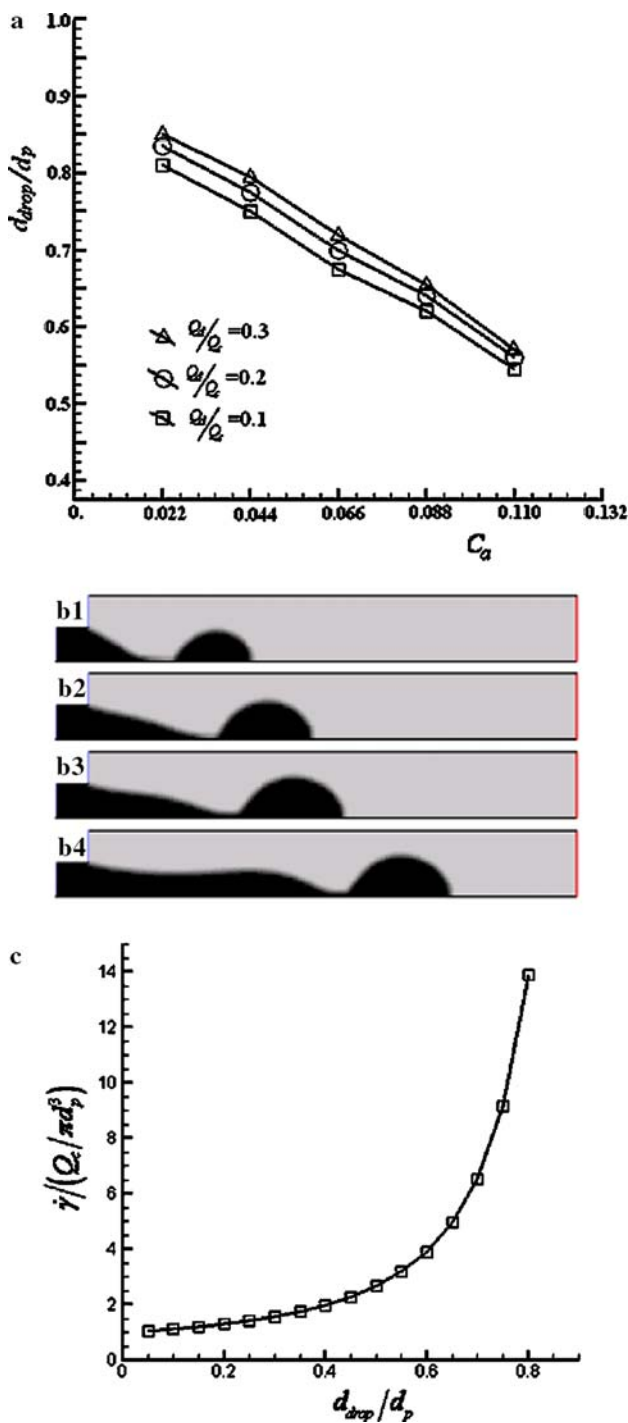


Fig. 2 Droplet generation with $Q_d/Q_c \geq 0.1$. **a** Droplet size increases with Q_d/Q_c very slowly at a constant value of Ca . The diameter change is less than 3% at $Q_d/Q_c = 0.2$ and 0.3 . **b** Interface profiles at $Ca = 0.0885$ with the flow rate ratios of **b1** $Q_d/Q_c = 0.02$, **b2** $Q_d/Q_c = 0.1$, **b3** $Q_d/Q_c = 0.2$ and **b4** $Q_d/Q_c = 0.3$. **c** The change of strain rate with the drop diameter. The curve slope becomes steep after $d_{drop}/d_p = 0.5$

In flow-focusing microfluidic systems, the average velocity at inlet was $u \approx 0.01\text{--}0.4$ m/s (Nisisako et al. 2003; Stone et al. 2004), while the velocity through a

narrow orifice was up to 1.7 m/s and the velocity of the disperse fluid could be as low as 10^{-5} m/s. So in this study of co-flowing microfluidic systems, the average velocity of the disperse fluid is $u_d \approx 0.001\text{--}0.5$ m/s and the average velocity of the continuous fluid is $u_c \approx 0.1\text{--}2.0$ m/s. Simulation results are presented in a dimensionless framework. The flow rate ratio for this axisymmetric device is defined as $Q_d/Q_c = \frac{u_d d_i^2}{u_c (d_p^2 - d_i^2)}$. The capillary number based on the continuous velocity is $Ca = \frac{\mu_c u_c}{\sigma}$. Nondimensional drop size is represented as d_{drop}/d_p . The Reynolds number based on the dispersed velocity is $Re = \frac{\rho_d u_d d_i}{\mu_d}$.

The velocity at the centerline in fully developed pipe flow has the maximum value, according to the celebrated Hagen–Poiseuille study (White 1991). If at the inlets the average velocity of the outer (continuous) fluid is greater than that of the inner (disperse) fluid, natural flow-focusing phenomena would happen in the pipe even without a confined orifice. So the basic mechanism of the co-flowing system is similar to that of a flow-focusing system (Garstecki et al. 2005) and the general rules studied below might be applied to flow-focusing channels. Although the specific or critical values may be different, these rules in co-flowing microfluidic devices would be helpful for droplet control in other microfluidic channels.

3 Results and discussion

General effects of flow rate on droplet formation are shown in Fig. 1. When the dispersed phase ($Re = 4$) flows into a quiescent, ambient fluid ($Ca = 0$), the jet surface grows larger and larger, which nearly touches the pipe wall, but no droplet breaks off from the tube. It only turns to a laminar flow, as shown in Fig. 1b. Increasing the capillary number, discrete droplets are formed as shown in Fig. 1c. Still increasing the values of Ca and Re , there is a long suspended column of the disperse fluid at the tube, as shown in Fig. 1d.

Detailed effects of flow rate on droplet formation are shown below. From the results of a large number of simulation cases, transition conditions are discovered in our study that the droplet size is either approximately independent of or strongly dependent on the flow rate ratio. When $Q_d/Q_c \geq 0.1$, droplet size is approximately independent of the flow rate ratio and the size decreases with the increase of Ca . It is very interesting that these data roughly follow quasilinear curves as shown in Fig. 2a, which makes droplet control convenient. This phenomenon is also explained from the relation between the strain rate and the drop diameter.

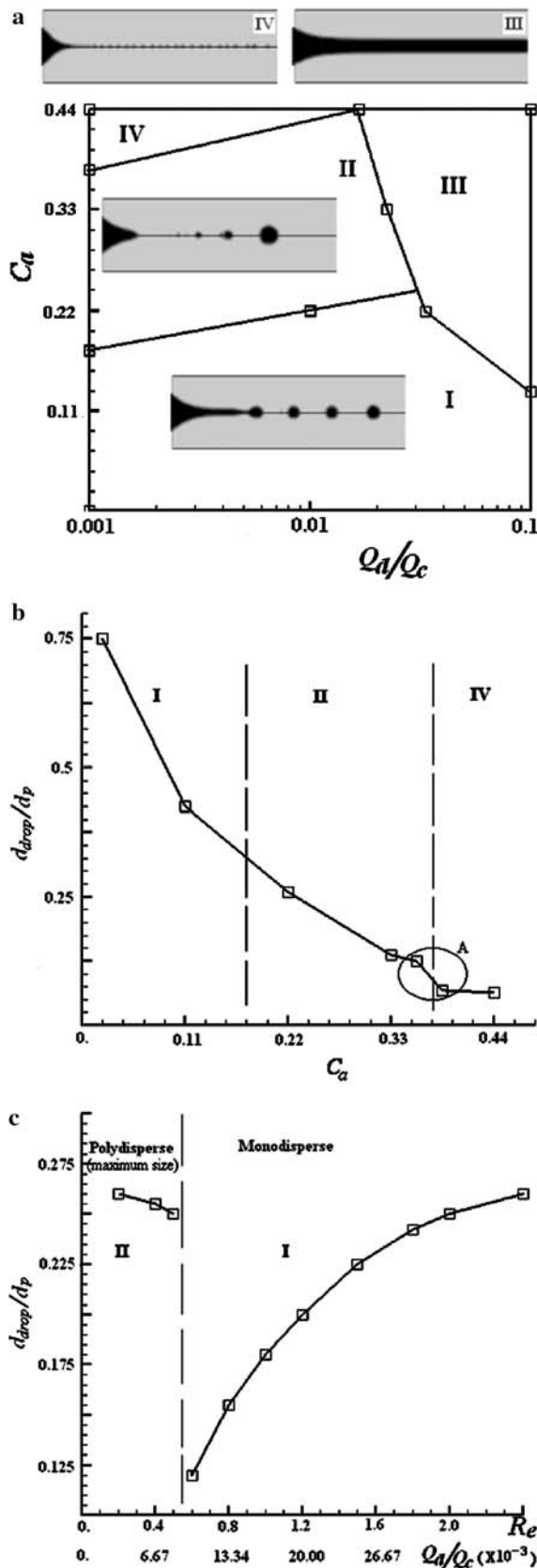


Fig. 3 a Demarcated regions for four drop patterns and images of four drop patterns with $Q_d/Q_c < 0.1$. Polydisperse pattern is avoided by choosing $Ca < 0.177$. Laminar flow pattern is avoided by choosing $Ca < 0.133$. b Droplet diameter distribution as a function of Ca at $Re = 0.2$. c Droplet diameter distribution as a function of Re and Q_d/Q_c at $Ca = 0.221$

The interface profiles at the instant when the droplets are just breaking up are shown in Fig. 2b. Two different drop formation mechanisms (Cramer et al. 2004; Utada et al. 2005) can be distinguished: the droplet in Fig. 2b1 is formed close to the capillary tip (dripping) and the droplet in Fig. 2b4 breaks up from an extended jet (jetting). At a constant value of Ca , the Reynolds number of the discrete phase increases with the flow-rate ratio, the length of liquid thread increases due primarily to the increase in the inertial force to elongate the liquid cone remaining on the tube. Even when the drop formation mechanisms has changed from dripping to jetting, only two tries of experiment are needed to define a quasilinear curve shown in Fig. 2a, thus it is quite convenient for droplet control in microfluidic systems. Taylor’s research (1932) can be used to explain this interesting phenomenon. Although numerical simulations eliminate restrictions on flow forms, analytical expressions under simplified flow conditions would be helpful to explain some simulation results. The predicted diameter of a droplet under the force due to viscosity and the force due to surface tension is (Taylor 1932)

$$d_{drop} = \frac{4\sigma(\mu_d + \mu_c)}{\dot{\gamma}\mu_c(\frac{19}{4}\mu_d + 4\mu_c)} \quad (1)$$

where $\dot{\gamma}$ is the strain rate. For an fully developed axisymmetric flow, the simple expression $\dot{\gamma} = |du/dr|$ for the strain rate can be derived (Hong et al. 2003). When the continuous phase flows around the droplet in the pipe, we have $|du| \sim Q_c/\pi d_p^2 [1 - (d_{drop}/d_p)^2]$ and $dr = 0.5d_p (1 - d_{drop}/d_p)$. So the strain rate of the continuous phase in the co-flowing microfluidic device is related to the drop diameter through

$$\dot{\gamma} \sim \frac{Q_c}{\pi d_p^3 [1 - (d_{drop}/d_p)^2] (1 - d_{drop}/d_p)} \quad (2)$$

The curve in Fig. 2c is the analytical results from Eq. 2. Droplet diameters in Fig. 2a are greater than the tube size ($d_t = 0.5d_p$). As shown in Fig. 2c, a little increase of d_{drop} may cause a great increase of $\dot{\gamma}$ with $d_{drop} > 0.5d_p$. Under this condition, a droplet with a

larger size tends to be formed with the increase of the flow rate ratio, but this causes the strain rate $\dot{\gamma}$ to increase very fast, which quickly leads to a disruptive force due to viscosity. Therefore when $Q_d/Q_c \geq 0.1$, a confined drop size is formed for a constant value of Ca , which is approximately independent of the flow rate ratio.

Drop generation frequency f from numerical results increases synchronously with Q_d for the range of $Q_d/Q_c \geq 0.1$. For example, the frequencies with $Ca = 0.0885$ at $Q_d/Q_c = 0.1$, $Q_d/Q_c = 0.2$ and $Q_d/Q_c = 0.3$ are $1/(210 \mu s)$, $1/(110 \mu s)$ and $1/(90 \mu s)$, respectively. The relationship between d_{drop} and f follows the following equation (Cramer et al. 2004)

$$d_{\text{drop}} = 3 \sqrt{\frac{6}{\pi} \cdot \frac{Q_d}{f}} \quad (3)$$

In the case of drop size is monodisperse, the above relationship is quite obvious from the continuity equation of the disperse phase.

The size of the encapsulated droplets strongly affects targeting efficiency in drug delivery (Nagayasu et al. 1999). Droplet diameters in this range ($Q_d/Q_c \geq 0.1$ and $Ca \leq 0.111$) are greater than the tube size. If the droplet size we want is smaller, we could choose parameters with $Q_d/Q_c < 0.1$.

From the results of a large number of simulation cases, when $Q_d/Q_c < 0.1$, droplet pattern and size are found to be strongly dependent on both the flow rate ratio and the capillary number. Droplet sizes in microfluidic systems can be tuned by adjusting the input flow rates. Unfortunately, this affects simultaneously the frequency, size and pattern of the droplets. To solve this difficulty in parameter selection, regions are demarcated for different drop patterns.

Four different patterns of droplet formation may occur with $Q_d/Q_c < 0.1$. From the results of 43 simulation cases, it is interesting to find that four corresponding regions can be demarcated as shown in Fig. 3a. Images for these patterns are also shown in Fig. 3a. The coefficient of variation (CV) is one important parameter to describe the patterns. The criterion $CV < 5\%$ is used to distinguish between monodisperse droplets and polydisperse droplets. In pattern I, monodisperse droplets or a primary drop with a very small satellite droplet are included. In the latter case, the volume ratio of the tiny satellite to the large droplet is in the range of $0 \sim 8^{-3}$. The satellite droplet can be omitted as its diameter is less than 0.5% that of the primary drop. Polydisperse droplets are formed in pattern II. Laminar flows are formed in pattern III. In pattern IV, only monodisperse droplets

are formed. Significantly increasing the capillary number of the continuous fluid, viscous stress exerted by the external fluid becomes so large that it squeezes the disperse fluid to form a very narrow thread, which allows formation of monodisperse droplets with diameters much smaller than the tube width.

Both dripping and jetting mechanisms exist in pattern I. When the surface tension force is exceeded by the composition of other forces, the drop necks and starts to detach from the remaining part of the disperse fluid on the tube. The tip (apex) part of the remaining fluid may recoil totally under the unbalanced force of surface tension and the case of monodisperse droplets is formed. If the tip part breaks under the action of higher inertial force and viscous force, the case of a primary drop accompanied by a tiny satellite droplet is formed (Ambravaneswaran et al. 2004). Increasing Ca under the same flow rate ratio, a long liquid thread may form during the necking sequence. This liquid thread connects the detaching drop and the remainder of the disperse fluid at the tube. Polydisperse pattern occurs as the thread breaks up at its both ends. If the Reynolds number base on the disperse fluid is increased at the same time, no drops but laminar flow forms in the pipe and it is shown as pattern III in this paper. Significantly increasing the capillary number of the continuous fluid, only monodisperse droplets are formed in pattern IV.

It is helpful to avoid polydisperse and laminar flow patterns with Fig. 3a. As shown in Fig. 3b, three patterns of droplets occur by changing Ca at $Re = 0.2$. There is a step change shown by the cycle “A” in the curve. This step is consistent with the change from pattern II to IV. Increasing the value of Ca , polydisperse droplets occur. At last monodisperse droplets of very small size are formed with $Ca > 0.365$.

The change of Re at $Ca = 0.221$ affects three types (II, I and III) of droplet patterns too, only two patterns are illustrated in Fig. 3c. Droplet diameter distribution is departed by a dashed line. Diameter in the left side is the value of the maximum droplet in polydisperse pattern. The route to get a droplet size we want is not unique. The minimum CV of the diameter is usually the first criterion. To get a droplet diameter of $d_{\text{drop}} = 0.25 d_p$ with Fig. 3c, control parameters from the right side of the dashed line is of course better than those from the left side.

Pattern I and II in Fig. 3a are widely shown in these existing experimental results on co-flowing devices (Ambravaneswaran et al. 2004; Cramer et al. 2004; Utada et al. 2005). As pattern III is a simple laminar flow, it should be avoided in selecting control parameters for droplet generation. In pattern IV, as monodisperse

droplets have diameters much smaller than the tube width, this could be of great interest for applications. The parameter space for pattern IV are $Ca > 0.365$ and $Q_d/Q_c \sim 10^{-3}$. The characteristic numbers Ca in the experiment can be determined by adjusting the velocity (Cramer et al. 2004) or the viscosity (Garstecki et al. 2005), the value of $Ca > 0.365$ is realistic in these experiments. The choice of $Q_d/Q_c \sim 10^{-3}$ is also realistic in the experiment of Dreyfus et al. (2003). So properly adjusting parameters as shown in Fig. 3a, the proposed drop pattern map will occur in reality.

4 Conclusion

An axisymmetric configuration is developed to produce both monodisperse and polydisperse droplets. Changing the flow rate ratio, there is a transition of two states. When $Q_d/Q_c \geq 0.1$, droplet size is approximately independent of the flow rate ratio. Diameter distribution on Ca is found to follow a quasi-linear curve which makes droplet control convenient. This interesting phenomenon could be explained from the relation between the strain rate and the drop diameter. When $Q_d/Q_c < 0.1$, the droplet size is strongly dependent on the flow rates. Droplet sizes in microfluidic systems can be tuned by adjusting the input flow rates. Unfortunately, this affects simultaneously the frequency, size and pattern of the droplets. To solve this difficulty in parameter selection, regions are demarcated for different drop patterns from the results of a large number of simulation cases. In pattern IV, as monodisperse droplets have diameters much smaller than the tube width, this could be of great interest for applications.

Acknowledgments The work is supported by NSFC (Project No: 10402044). We are grateful to Zhizhong Li for many inspiring discussions.

References

Ambravaneswaran B, Subramani HJ, Phillips SD, Basaran OA (2004) Dripping-jetting transitions in a dripping faucet. *Phys Rev Lett* 93:034501

- Cramer C, Fischer P, Windhab EJ (2004) Drop formation in a co-flowing ambient fluid. *Chem Eng Sci* 59:3045–3058
- Day D, Gu M (2005) Microchannel fabrication in PMMA based on localized heating by nanojoule high repetition rate femtosecond pulses. *Opt Express* 13:5939–5946
- Dreyfus R, Tabeling P, Willaime H (2003) Ordered and disordered patterns in two-phase flows in microchannels. *Phys Rev Lett* 90:144505
- Gadelhak M (2000) *Flow control*. Cambridge University Press, Cambridge
- Ganan-Calvo AM, Gordillo JM (2001) Perfectly monodisperse microbubbling by capillary flow focusing. *Phys Rev Lett* 87:274501
- Garstecki P, Fuerstman MJ, Whitesides GM (2005) Nonlinear dynamics of a flow-focusing bubble generator: an inverted dripping faucet. *Phys Rev Lett* 94:1–4
- Hong YP, Li HX (2003) Comparative study of fluid dispensing modeling. *IEEE Trans Electron Packag Manuf* 26:273–280
- Jensen MJ, Stone HA, Bruus H (2006) A numerical study of two-phase Stokes flow in an axisymmetric flow-focusing device. *Phys Fluids* 18:077103
- Joanicot M, Ajdari A (2005) Droplet control for microfluidics. *Science* 309:887–888
- Li D (1996) Drop size dependence of contact angles and line tensions of solid-liquid systems. *Colloids Surf A* 116:1–23
- Nagayasu A, Uchiyama K, Kiwada H (1999) Size of liposomes: a factor which affects their targeting efficiency to tumors and therapeutic activity of liposomal antitumor drugs. *Adv Drug Deliv Rev* 40:75–87
- Nisisako T, Toru T, Toshiro H (2003) Rapid preparation of monodispersed droplets with confluent laminar flows. *Proc IEEE Micro Electro Mech Syst (MEMS)* 331–334
- Richards JR, Beris AN, Lenhoff AM (1995) Drop formation in liquid-liquid systems before and after jetting. *Phys Fluids* 7:2617–2630
- Stone HA, Stroock AD, Ajdari A (2004) Engineering flows in small devices: microfluidics toward a lab-on-a-chip. *Annu Rev Fluid Mech* 36:381–411
- Suryo R, Basaran OA (2006) Tip streaming from a liquid drop forming from a tube in a co-flowing outer fluid. *Phys Fluids* 18:082102
- Taylor GI (1932) The viscosity of a fluid containing small drops of another fluid. *Proc R Soc A* 138:41–47
- Thorsen T, Roberts RW, Arnold FH, Quake SR (2001) Dynamic pattern formation in a vesicle-generating microfluidic device. *Phys Rev Lett* 86:4163–4166
- Utada AS, Lorenceau E, Link DL, Kaplan PD, Stone HA, Weitz DA (2005) Monodisperse double emulsions generated from a microcapillary device. *Science* 308:537–541
- White FM (1991) *Viscous fluid flow*. McGraw-Hill, New York
- Zhang X (1999) Dynamics of drop formation in viscous flows. *Chem Eng Sci* 54:1759–1774